



Title	Decreased amyloid- pathologies by intracerebral loading of glycosphingolipid-enriched exosomes in Alzheimer model mice
Author(s)	Yuyama, Kohei; Sun, Hui; Sakai, Shota; Mitsutake, Susumu; Okada, Megumi; Tahara, Hidetoshi; Furukawa, Jun-Ichi; Fujitani, Naoki; Shinohara, Yasuro; Igarashi, Yasuyuki
Citation	Journal of Biological Chemistry, 289(35), 24488-24498 <a href="https://doi.org/10.1074/jbc.M114.577213">https://doi.org/10.1074/jbc.M114.577213</a>
Issue Date	2014-08
Doc URL	<a href="http://hdl.handle.net/2115/57658">http://hdl.handle.net/2115/57658</a>
Rights	This research was originally published in Journal Name: Journal of biological chemistry Author(s). Title: Decreased amyloid- pathologies by intracerebral loading of glycosphingolipid-enriched exosomes in Alzheimer model mice Journal Name. Year: 2014. Vol: 289(35) 24488-98 © 2014 the American Society for Biochemistry and Molecular Biology
Type	article (author version)
File Information	JBC_M114.577213--2.pdf



[Instructions for use](#)

## Decreased Amyloid- $\beta$ Pathologies by Intracerebral Loading of Glycosphingolipid-enriched Exosomes in Alzheimer Model Mice

Kohei Yuyama<sup>1</sup>, Hui Sun<sup>1</sup>, Shota Sakai<sup>1</sup>, Susumu Mitsutake<sup>1,2</sup>, Megumi Okada<sup>3</sup>, Hidetoshi Tahara<sup>3</sup>, Jun-ichi Furukawa<sup>4</sup>, Naoki Fujitani<sup>4</sup>, Yasuro Shinohara<sup>4</sup>, and Yasuyuki Igarashi<sup>1</sup>

From <sup>1</sup>Laboratory of Biomembrane and Biofunctional Chemistry, Graduate School of Advanced Life Science, and Frontier Research Center for Post-Genome Science and Technology, Hokkaido University, Sapporo 001-0021, Japan.

<sup>2</sup>Department of Applied Biochemistry and Food Science, Faculty of Agriculture, Saga University, Saga 840-8502, Japan.

<sup>3</sup>Department of Cellular and Molecular Biology, Graduate School of Biomedical Science, Hiroshima University, Hiroshima 734-8553, Japan

<sup>4</sup>Laboratory of Medical and Functional Glycomics, Graduate School of Advanced Life Science, and Frontier Research Center for Post-Genome Science and Technology, Hokkaido University, Sapporo 001-0021, Japan.

**\*Running title:** Exosome-mediated A $\beta$  clearance in AD mouse brains

To whom correspondence should be addressed: Yasuyuki Igarashi, Laboratory of Biomembrane and Biofunctional Chemistry, Graduate School of Advanced Life Science, and Frontier Research Center for Post-Genome Science and Technology, Hokkaido University, Kita21 Nishi11, Sapporo 001-0021, Japan. Tel: +81(11)-706-9001; FAX +81(11)-706-9087; E-mail: yigarash@pharm.hokudai.ac.jp

Keywords: exosome; amyloid-beta (A $\beta$ ); Alzheimer disease; glycosphingolipid

**Background:** Exosome, a type of extracellular vesicles, can associate with A $\beta$  in vitro.

**Results:** Intracerebrally injected exosomes trapped A $\beta$  on surface glycosphingolipids and transported it into microglia in AD mouse brains, resulting in reductions in A $\beta$  pathology.

**Conclusion:** Exogenous exosomes act as potent scavengers for A $\beta$  in mouse brains.

**Significance:** The findings provide a novel therapeutic approach for AD.

### ABSTRACT

Elevated levels of amyloid- $\beta$  peptide (A $\beta$ ) in the human brain are linked to the pathogenesis of Alzheimer disease (AD). Recent in vitro

studies have demonstrated that extracellular A $\beta$  can bind to exosomes, which are cell-secreted nanovesicles with lipid membranes that are known to transport their cargos intercellularly. Such findings suggest that the exosomes are involved in A $\beta$  metabolism in brain. Here, we found that neuroblastoma-derived exosomes exogenously injected into mouse brains trapped A $\beta$  and with the associated A $\beta$  were internalized into brain-resident phagocyte microglia. Accordingly, continuous intracerebral administration of the exosomes into amyloid- $\beta$  precursor protein (APP) transgenic mice resulted in marked reductions in A $\beta$  levels,

**amyloid depositions, and A $\beta$ -mediated synaptotoxicity in the hippocampus. In addition, we determined that glycosphingolipids (GSLs), a group of membrane glycolipids, are highly abundant in the exosomes, and the enriched glycans of the GSLs are essential for A $\beta$  binding and assembly on the exosomes, both in vitro and in vivo. Our data demonstrate that intracerebrally administered exosomes can act as potent scavengers for A $\beta$  by carrying it on the exosome surface GSLs, and suggest a role of exosomes in A $\beta$  clearance in the central nervous system. Improving A $\beta$  clearance by exosome administration would provide a novel therapeutic intervention for AD.**

Alzheimer disease (AD), a common dementia, is pathologically characterized by the presence of amyloid- $\beta$  peptide (A $\beta$ )-containing senile plaques within the brain. In familial AD, genetic mutations cause increased production of A $\beta$  (1), whereas in far more common sporadic cases, A $\beta$  generation is normal, but its clearance is impaired (2). Elevated levels of A $\beta$ , caused by an imbalance in its metabolism, are linked to synaptic and nerve loss, which likely manifest as progressive cognitive deficits in AD (3).

Exosomes represent a subtype of secreted membrane vesicles (40-100 nm in diameter) of endosomal origin that are released from various types of cells including neurons (4). Exosomes serve to remove and discard unwanted proteins into a drainage system; they are also known to intercellularly shuttle their cargo: a specific set of proteins, RNAs, and lipids (5). Recently, exosomes were reported to associate with a portion of extracellular amyloid- $\beta$  precursor protein (APP) and its metabolites, including C-terminal fragments (CTFs), amyloid intracellular domain (AICD), and A $\beta$ , in cultures of human wild-type or mutant human

APP-expressing neuroblastoma cells (6,7). In addition, exosomal proteins such as Alix and flotillin-1 were identified around neuritic plaques in AD brains (6). Similarly, our previous study demonstrated that exosomes released from neuroblastoma or primary cortical neurons can bind to synthetic or endogenous A $\beta$ , and promote A $\beta$  fibril formation on their surface in vitro (8). Furthermore, exosome-bound A $\beta$  is incorporated into microglia for degradation, suggesting that exosomes may act as a mediator for A $\beta$  elimination in brains (8). Here, we demonstrated that long-term intracerebral administration of exosomes to the brain of APP transgenic mice resulted in a marked reduction in A $\beta$  levels, amyloid depositions and A $\beta$ -mediated synaptotoxicity. We also clarified that glycosphingolipids (GSLs) abundant in the exosomes were essential for A $\beta$  binding on the exosome surface.

## **EXPERIMENTAL PROCEDURES**

*Cell cultures* - Murine neuroblastoma Neuro2a (N2a) cells were maintained in Dulbecco's modified Eagle's medium (Invitrogen, Carlsbad, CA) supplemented with 10% fetal bovine serum. The murine microglial cell line BV-2 was purchased from National Cancer Institute (Istituto Nazionale per la Ricerca sul Cancro, Genova, Italy) and was cultured in RPMI1640 (Invitrogen) supplemented with 10% fetal bovine serum and 2 mM L-glutamine.

*Animals* - All animal experiments were conducted under a protocol approved by the animal care committees of Hokkaido University. Wild type C57BL/6 mice were purchased from Japan SLC Inc. (Hamamatsu, Japan). Heterozygotic transgenic mice that express the human APP bearing the Swedish and Indiana (KM670/671NL, V717F) mutations (APP<sub>sweInd</sub> or J20 strain) were from the Jackson Laboratory (Bar

Harbor, ME) and maintained in barrier facilities.

*Exosome isolation* - Exosomes were prepared from culture supernatants of N2a cells as described previously (9). Briefly, one day before exosome isolation, culture medium was replaced with serum-free medium. The culture supernatants were collected and sequentially centrifuged at 3,000g for 10 min, at 4,000g for 10 min, and at 10,000g for 30 min to remove cells, dead cells, and debris, then spun again at 100,000g for 1 hour to obtain exosomes as pellets.

For sucrose gradient analysis, each exosome pellet (100 µg protein) was loaded onto 10 ml of a sucrose gradient (0.25-2.3M sucrose in 20 mM HEPES, 10 ml) and centrifuged at 100,000g for 18 h. After centrifugation, 1 ml fractions were collected, diluted with 20 mM HEPES, and precipitated by centrifugation for 1 hour at 100,000g. The resulting pellets were resuspended in PBS and subjected to Western blot analysis.

*Electron microscopy* - Exosomes (100 µg protein/ml) were re-suspended in 50 mM Tris/150 mM NaCl buffer, pH 7.6 (TBS) and applied to a grid covered with collodion. For A $\beta$  binding experiments exosomes (100 µg protein/ml) were incubated with A $\beta$ <sub>1-42</sub> (15 µM) in TBS at 37 °C for 5 h after pre-treating with or without EGCase. Exosome mixtures were then applied to the grid. Exosomes were negatively stained with 2% phosphotungstic acid. Transmission images were acquired using an HD-2000 (Hitachi, Tokyo, Japan) or JEM-1400Plus (JEOL Ltd. Tokyo, Japan) transmission electron microscope.

*Dynamic light scattering* - Exosomes (untreated or treated with EGCase) were suspended in TBS at 100 µg protein/ml. The particle size of the exosomes was measured by dynamic light scattering using a DelsaNano HC (Beckmann Coulter).

*Injection and isolation of biotinylated exosomes* - Exosomes were biotinylated with EZ-link

sulfo-NHS Biotin (Pierce, Rockford, IL), according to the manufacturer's protocol with minor modifications. Briefly, the exosomes were suspended in PBS (150 µg protein/ml) and incubated with biotin reagent (1 mg/ml) at room temperature for 30 min. The biotinylated exosomes were isolated by ultracentrifugation at 100,000g for 1h at 4°C, and re-suspended in PBS. For detecting co-precipitated A $\beta$ , two microliter of the 5 µg/µl biotin-exosome solution was injected into the right hippocampus of APP mouse (4-month-old) using stereotaxic coordinates and keep for 3h. The biotinylated exosomes in the homogenates of the hippocampus were precipitated using streptavidin microbeads according to the protocol in a µMACS streptavidin kit (Miltenyi Biotech, Bergisch Gladbach, German). Co-precipitated A $\beta$  was analyzed with Western blotting or ELISA following the solubilization of the exosomes in SDS sample buffer or guanidine buffer, respectively.

*SDS-PAGE and Western blotting* - SDS-PAGE and Western blot analysis were performed according to the standard methods of Laemmli. To detect target proteins, we employed as a primary antibody monoclonal antibodies against Alix (BD Bioscience, San Jose, CA), APP CTFs (Sigma), actin (Sigma), A $\beta$  (6E10, Signet, Dedham, MA), or neprilysin (Santa Cruz Biotechnology), or rabbit polyclonal antibodies against flotillin-1, endothelin converting enzyme (ECE)-1, (Santa Cruz Biotechnology) or insulin degrading enzyme (IDE, abcam), and as a secondary antibody an anti-mouse IgG-HRP antibody (GE Healthcare), or anti-rabbit IgG-HRP antibody (GE Healthcare). To detect the ganglioside GM1, we used horse radish peroxidase (HRP)-conjugated cholera toxin B subunit (CTB) from Sigma. Bands were visualized using a combination of an ECL Plus kit (GE Healthcare) and an LAS4000 imaging system

(Fuji Film, Tokyo).

*Fluorescence labeling for the exosomes* - Exosomes were stained with the red fluorescence dye PKH26 (Sigma) as described previously (8). Briefly, the exosomes were re-suspended in diluent C (Sigma) and incubated with PKH26 at room temperature for 5 minutes. The reaction was stopped by addition of 1% bovine serum albumin. The PKH26-labeled exosomes were precipitated again by ultracentrifugation at 100,000g at 4°C for 1 hour.

*Exosome isolation from murine CSF* - CSF was collected from the cisterna magna of 2-month-old C57BL/6 mice as previously described (10). Exosomes were isolated from the CSF using a method similar to that described above for isolation from culture medium.

*Analysis of exosomal particle number* - A qNano System (Izon Science, Ltd) was employed to analyze the particle densities of N2a- and mouse CSF-derived exosomes resuspended in PBS.

*Exosome administration in mouse brains* - Mice were continuously treated with exosome solution (2 mg protein/ml) or vehicle (PBS) by Alzet minipump (model 1002) at 0.25  $\mu$ l/h for 14 days. Mice were placed in a stereotactic instrument (NARISHIGE, Tokyo, Japan) and stainless steel cannulas of Alzet Brain Infusion Kit3 were implanted into the right lateral ventricle (mediolateral, -0.8 mm; dorsoventral -3.0 mm) or hippocampus (anteroposterior, -2.0 mm; mediolateral, -1.3 mm; dorsoventral -2.2 mm). After 14-day infusion, mice were then transcardially perfused with cold heparin/PBS. The right hemisphere was fixed with 4% paraformaldehyde/PBS at 4°C for 48h for use in immunohistochemistry, and the left hemisphere was rapidly frozen with liquid nitrogen and stored at -80°C for later analysis.

For single injection studies, PKH-labeled

exosomes or a conjugate of PKH-exosomes with fluorescent A $\beta$  (4  $\mu$ g exosome protein in 2 $\mu$ l PBS) were injected into the right hippocampus or the lateral ventricle of non-transgenic mice using stereotaxic coordinates as described above. To obtain the conjugates of the exosomes with A $\beta$ , PKH-exosomes (100  $\mu$ g/ml) were incubated with A $\beta$ <sub>1-40</sub> in TBS at 37°C for 24h, then centrifuged at 100,000g for 1h to remove free A $\beta$ . At 3 or 24h post injection, the mouse brains were prepared as described above for immunohistochemistry.

*Immunohistochemistry* - The tissue sections were cut with a cryostat (Leica CM3050S) and post-fixed with 4% paraformaldehyde/PBS. After a blocking with 5% BSA, 16  $\mu$ m-thick sections were immunostained with monoclonal antibodies against, Iba1 (Wako),  $\beta$ III tubulin (Promega), or glial fibrillary acidic protein (GFAP, SHIMA laboratory), followed by visualization with AlexaFluor488-conjugated anti-IgG. Serial 30  $\mu$ m-thickness of brain sections were immunostained with monoclonal antibody against A $\beta$  (4G8, Covance) after a brief formic acid treatment and the signals were visualized using ABC elite kit (Vector Laboratories). Confocal images were obtained using an Olympus Fluoview FV10i microscope. The A $\beta$  plaques were estimated as the percentage of the immunopositive area (positive pixel) to the examined area (total pixel) using ImageJ software.

*A $\beta$  ELISA* - A $\beta$  levels were determined using a sandwich enzyme-linked immunosorbent assay (ELISA). The kits for A $\beta$ <sub>1-40</sub> and A $\beta$ <sub>1-42</sub> were obtained from Wako (Osaka, Japan), and that for A $\beta$ <sub>1-38</sub> was from IBL (Gunma, Japan). Mouse hippocampus or exosomes were homogenized in 4M guanidine-HCl buffer (pH 8.0) with an ultrasonic homogenizer (TAITEC, Saitama, Japan). After incubation at room temperature for 3 h, the homogenates were further diluted with 0.1% BSA/PBS and centrifuged at 16,000g for 20min.

The resulting supernatants were then applied to the ELISA. All samples were measured in duplicate.

*Evaluation of synaptic densities* - Synaptophysin-immunoreactive synaptic densities were quantified according to the methods of Mucke et al (11) with minor modifications. The right hemisphere of each APP mouse brain was sagittally cut into 16  $\mu\text{m}$ -thick sections using a freezing microtome. The serial sections were incubated with a monoclonal antibody against synaptophysin (D35E4, Cell Signaling), followed by incubation with AlexaFluor488-bound anti-IgG. Immunofluorescent signals were visualized using an Olympus Fluoview FV10i microscope. The linear range of the synaptophysin-positive fluorescence intensities in nontransgenic control sections was determined, and the same setting was used to analyze all of the following images. For each mouse, 9 confocal images were captured in three sections per right hemisphere of the brain, and each image covered an area  $5500 \mu\text{m}^2$  in the molecular layer of the dentate gyrus. The synaptophysin-immunoreactive synaptic densities were estimated as a percentage of the immunostained area (positive pixel) to the selected image area (total pixel) using ImageJ software.

*Thioflavin-S (ThS) staining* - Brain sections (30  $\mu\text{m}$  thick) were oxidized with 0.25% potassium permanganate for 20 min followed by 3 min bleaching in 2% potassium metabisulfite and 1% oxalic acid. Sections were stained with 0.015% ThS in 50% ethanol in the dark for 10 min. After developing in two changes of 50% ethanol for 4 min each, images were captured with Olympus Fluoview FV10i microscope, and ThS-positive plaques were counted in three sections per mouse hippocampus.

*Measurement of Glycosphingolipids (GSLs)* - The extraction of GSLs from the culture cells and

the exosomes, the enzymatic digestion of GSL-glycans with EGCCase I and II (Takara Bio, Shiga, Japan), and the purification of glycans using glycoblotting were performed as described previously (12). Purified GSL-glycans were analyzed by MALDI-TOF MS using an Ultraflex II TOF/TOF mass spectrometer equipped with a reflector, which was controlled by the FlexControl 3.0 software package (Bruker Daltonics, Bremen, Germany). All spectra were obtained as positive ions and were annotated using the FlexAnalysis 3.0 software package (Bruker Daltonics). The glycan structures were then identified by online database SphinGOMAP<sup>®</sup> (<http://www.sphingomap.org/>).

*Quantification of Chol, SM, Cer, and PC* - Total lipids were extracted from the exosomes or N2a cells by adding chloroform/methanol (1:2, v/v). Levels of sphingomyelin (SM) and ceramide (Cer) were determined by electron ionization-mass spectrometry (TripleTOF<sup>TM</sup> 5600) coupling with PeakView software (AB SCIEX, Framingham, MA). Cer (C16:0, d18:1) and SM (C16:0, d18:1) were purchased from Avanti Polar Lipid (Alabaster, AL) and were used as standards. The amounts of phosphatidylcholine (PC) and cholesterol (Cho) were measured by a phosphatidylcholine assay kit (BioVision, Milpitas, CA) and cholesterol E-test kit (Wako), respectively.

*Proinflammatory cytokine ELISA* - The levels of proinflammatory cytokines, including tumor necrosis factor (TNF- $\alpha$ ), interleukin (IL)-6, IL-1 $\beta$ , and interferon (IFN)- $\gamma$  were determined by ELISA (Multi-Analyte ELISArray, Qiagen) according to the manufacturer's instructions. Briefly, each APP mouse hippocampus was homogenized in 4M guanidine-HCl buffer (pH 8.0) using an ultrasonic homogenizer (TAITEC, Saitama, Japan). After an incubation at room temperature for 3 h, the homogenates were further

diluted in 0.1%BSA/PBS, and centrifuged at 16,000g at 4°C for 20min. The resulting supernatant were applied to the ELISA. All samples were handled in duplicate.

*Endoglycosylceramidase (EGCase) and sialidase treatment* - Exosomes (1 mg protein/ml) were incubated with 0.5U/ml EGCase II (Takara Bio Inc., Shiga, Japan) at 37°C for 15 h in PBS containing 20 mM HEPES (pH 7.4), or 1U/ml sialidase from *Clostridium perfringens* (Sigma) at 37°C for 16 h in 50 mM acetate buffer (pH 5.5). Each mixture was centrifuged at 100,000 g for 1 h. The resultant precipitates were resuspended in TBS or HBS buffer and used for further examination.

*Seed-free A $\beta$  preparation* - Seed-free A $\beta$  solutions were prepared essentially according to a published report (13).

*A $\beta$  binding assay* - PKH26-labeled exosomes (untreated or treated with EGCase) were plated on chamber slideglass (Thermo Fisher Scientific, Waltham, MA) by staying in PBS for 1h at RT. Fluorescence-labeled A $\beta_{1-42}$  (1  $\mu$ M) was then added into the chamber of cultured N2a cells or the labeled exosomes and co-incubated in serum-free medium at 37°C for 5 h. After a wash with PBS to remove free A $\beta$ , fluorescent images were captured using Olympus Fluoview FV10i microscope.

*Binding analysis by surface plasmon resonance (SPR)* - The binding studies of N2a-derived exosomes (untreated, or pretreated with EGCase) with immobilized A $\beta$  peptide (A $\beta_{1-40}$ , A $\beta_{1-42}$ , A $\beta_{1-38}$  or A $\beta_{42-1}$ ) were performed using BIACORE T200 instrument (GE Healthcare). Briefly, seed-free A $\beta$  was independently immobilized onto a carboxymethylated (CM) dextran-coated gold surface (CM5 sensor chip) by amine coupling. The amount (RU) of immobilized A $\beta_{1-40}$ , A $\beta_{1-42}$ , A $\beta_{1-38}$  or A $\beta_{42-1}$  was 1143.0, 1266.7, 1316.3 or 948.0, respectively. Then the exosomes were

suspended in HBS buffer (10 mM HEPES, 150 mM NaCl, pH 7.4) and injected over the surface at 25 °C for one minute at a flow rate of 30  $\mu$ l/min. The resultant responses were subtracted from a blank that was immobilized with bovine serum albumin (BSA) or prepared by ethanolamine deactivation. Finally, the exosomes were regenerated from the A $\beta$ -immobilized surface by injecting 5 M guanidine-HCl, 10 mM Tris-HCl (pH 8.0).

*Thioflavin T (ThT) assay* - Seed-free A $\beta_{1-42}$  solutions (15  $\mu$ M) were incubated at 37°C for various times with the exosomes (100  $\mu$ g protein of exosomes in 100 $\mu$ l TBS), which had been untreated or treated with EGCase. Fluorescence intensities of ThT (Sigma) were determined as described before (8) using an Appliskan spectrofluorophotometer (Thermo Fisher Scientific).

*Exosome uptake assay* - Uptake of PKH26-labeled exosomes into microglial BV-2 cells were measured as described previously (8). Briefly, fluorescent exosomes were administered to BV-2 cells and incubated for various times in serum-free conditions. After a wash, the cells were then fixed, and confocal images were acquired using an Olympus Fluoview FV10i microscope. The fluorescence intensity of each samples was analyzed with ImageJ software.

## RESULTS

*Exogenously injected exosomes trap A $\beta$  and are incorporated into microglia in mouse brains* - To explore the hypothesis that providing exogenous exosomes in vivo would enhance A $\beta$  clearance by facilitating engulfment of exosome-bound A $\beta$  by microglia, we loaded isolated exosomes into mouse brains and evaluated the effect on the balance of A $\beta$  metabolism. Exosomes were collected from culture supernatants of mouse neuroblastoma

Neuro2a (N2a) cells using sequential ultracentrifugation; the exosomes typically consisted of membrane vesicles of 70-120 nm in diameter (Fig. 1A and B) as previously described (14). The presence of exosomes was confirmed by detecting the exosomal markers Alix and flotillin-1 as well as the membrane glycolipid GM1 ganglioside, in sucrose density gradient fractions corresponding to a density of 1.12 and 1.16 g/ml (Fig. 1C). A $\beta$  was not identified in N2a cells and the exosomes used in this study (Fig. 1C). Exosomes isolated from N2a cells were biotinylated and injected into the hippocampus of APP<sub>SweInd</sub> transgenic (APP) mice. Hippocampal A $\beta$  was detectable in streptavidin-precipitated exosomes, together with the marker Alix, 3 h after the injection (Fig. 1D). Accompanied by A $\beta$ , the intrahippocampal-injected exosomes co-localized with the microglial marker Iba1 (Fig. 1E), agreeing with our previous in vitro study (8). These results demonstrate that in mouse brains exogenous exosomes bind A $\beta$  and are then incorporated into microglia, together with the bound A $\beta$ , for degradation.

*Continuous exosome administration ameliorates A $\beta$  pathology and synaptic dysfunction in APP mouse brains* - we next continuously administered exosomes into the lateral ventricles of 4-month-old APP mice for 14 days using osmotic minipumps. The exosome solution (2 mg protein/ml) contained  $2.67 \times 10^{12}$  particles/ml, which is  $\sim 35$  times higher than the concentration of the exosomes in mouse cerebrospinal fluid (CSF) ( $7.51 \times 10^{10}$  particles/ml). The intraventricularly injected exosomes have been reported to penetrate into brain parenchyma (15). After two weeks, there was an approximate 50% reduction in total A $\beta_{1-40}$  and A $\beta_{1-42}$  levels and 35% reduction in A $\beta_{1-38}$  levels in the hippocampus of the exosome-treated APP mice, compared to those infused with vehicle (Fig. 2A). A similar

decline in A $\beta$  levels was confirmed by direct administration of the exosomes into mouse hippocampus, with  $\sim 50\%$  less observed in the ipsilateral injection side than the contralateral (Fig. 2B). APP mice given vehicle treatment exhibited approximately 50% decreased densities in synaptophysin immunoreactivities in the hippocampus, as compared to wild-type mice (Fig. 2C and D), agreeing with previous reports (11). After a 14-day-infusion of the exosomes, the synaptophysin immunoreactivities were markedly increased in the APP mouse hippocampus (85% and 50% of those observed in WT mice, following exosome and PBS treatment, respectively; Fig. 2D). Thus, the exosomes mediated significant recovery from synaptic impairment in the APP mice. Taken together, these findings validated that in vivo, exogenously added exosomes induce reductions in A $\beta$  levels and A $\beta$ -associated synaptotoxicity.

To assess the effect of exogenous exosomes on brain amyloid deposition, we continuously administered the exosomes into the hippocampus of 13-month-old APP mice for 14 days. We found that the exosomes markedly decreased the A $\beta$  immunoreactive burden (65% reduction; Fig. 3A and B) and number of thioflavin-S-positive plaques (38%; Fig. 3C) in the treated hippocampus, compared with the untreated side. Supporting these histological results, tissue levels of A $\beta_{1-40}$  and A $\beta_{1-42}$  were also significantly decreased following exosome infusion, as determined by ELISA (Fig. 3D). We also performed exosome infusion into the lateral ventricles of 13-month-old APP mice for 14 days and found significant reductions in A $\beta_{1-40}$  and A $\beta_{1-42}$  levels in the mouse hippocampus (Fig. 3E). These findings demonstrate the evident efficacy of long-term treatment with exogenous exosomes in A $\beta$  deposition, even deposition of the fibrillar species of A $\beta$  aggregates, in APP mice.

To exclude the possibility that the changes observed *in vivo* are due to effects of exosomes on A $\beta$  generation and enzymatic degradation, we examined the expression levels of APP and its cleaved fragments, including CTF- $\alpha$  and CTF- $\beta$ , in the hippocampus. No obvious differences in the expression levels were apparent between the exosome- and PBS-treated APP mice (Fig. 4A). In addition, the expression levels of well-known proteases for A $\beta$  peptides, including insulin-degrading enzyme (IDE), neprilysin (NEP), and angiotensin-converting enzyme (ACE), were investigated, but there were no variations even after exosome infusion (Fig. 4A). Although the exogenous exosomes were taken up by the microglia, there was no obvious activation in releasing the proinflammatory cytokines like tumor necrosis factor  $\alpha$  (TNF $\alpha$ ), interleukin (IL)-6, IL-1 $\beta$ , or interferon (IFN)- $\gamma$  in the exosome-treated mouse hippocampus (Fig. 4B). The above findings indicate that the exosomes reduce A $\beta$  levels by promoting an alternative pathway for A $\beta$  clearance, *i.e.*, exosome-associated A $\beta$  uptake by microglia, without any stimulation in APP processing, A $\beta$  degradation, or microglial inflammatory reactions.

*Exosomal GSL-glycans are critical for their association with A $\beta$  in vitro and in vivo* - The above experiments clearly indicate that the exogenous exosomes associated with the A $\beta$  in the mouse brains, although how they interact with each other remained to be determined. Increasing evidence with synthetic liposomes or membranes has demonstrated that gangliosides (sialic acid-containing GSLs) clustering on the membrane surface bind to A $\beta$ , and that this A $\beta$ -GSL complex then acts as a template for catalyzing the reaction of A $\beta$  fibril formation (16,17). *In vivo*, the monosialoganglioside GM1 was found to associate with A $\beta$  in human brains that exhibit AD pathology (18,19). GSLs are

reported to exist in exosomes (6), but details regarding which species of GSLs have not yet been described. We summarized the profiles of GSL-derived glycans from the exosomes and the cells from which the exosomes derived, by quantitative GSL-glycomics (Table 1). The total amount of GSLs was much higher in exosomes than in the parent cells (~2,300%, Fig. 5A). In either, the vast majority of GSLs were GM2 (>84%), with distinct minor compositions (Table 1). Except for GM2, the levels of sialylated GSLs were much higher in the exosomes (Fig. 5B). To investigate whether the GSLs abundant in the exosomes might affect A $\beta$  binding and fibril formation, we deglycosylated exosomal GSLs using endoglycoceramidase (EGCase), which specifically cleaves the linkage between the oligosaccharide and glucosylceramide in GSLs (20). The particle size of the exosomes was stable up to 5 h after EGCase digestion, though larger aggregates commonly formed during the 24 h-incubation (Fig. 5C). Within the 5 h-period, the EGCase-treated exosomes associated very little with the A $\beta$ , as compared to intact exosomes, which overtly colocalized with the A $\beta$  (Fig. 5D).

We performed surface plasmon resonance (SPR) studies to evaluate the specificity of the interaction between N2a-derived exosomes and individual A $\beta$ s. As shown in Fig. 5E, when the exosomes were injected onto the immobilized A $\beta$ <sub>1-42</sub> and A $\beta$ <sub>42-1</sub>, a peptide with reverse sequence of A $\beta$ <sub>1-42</sub>, only the former gave a significant increase in resonance signal, demonstrating the specific nature of the interaction. Specific interactions of the exosomes were observed not only with immobilized A $\beta$ <sub>1-42</sub> but also with A $\beta$ <sub>1-40</sub> and A $\beta$ <sub>1-38</sub>, and we found that the interactions were almost completely diminished when the exosomes were pretreated with EGCase (Fig. 5F). These results suggest that A $\beta$ s directly bind to the exosomes through the GSL glycans, particularly

those sialic acid moieties on their surface. Pre-treatment with EGCCase also inhibited exosome-dependent amyloid fibril formation in incubation mixtures of exosomes and A $\beta$ <sub>1-42</sub>, as assessed by thioflavin-T assay and electron microscopic observation (Fig. 6A and B). Cleavage of sialic acids with sialidase resulted in similar reductions in fibril formation (Fig. 6C). Steric blocking of GM1 or GM2 ganglioside by cholera toxin subunit B (CTB) or anti-GM2 antibody, respectively, also partially but significantly suppressed amyloid formation (Fig. 6C). In contrast to intact exosomes, the EGCCase-treated exosomes nearly failed to coprecipitate with A $\beta$  when injected into the hippocampus of APP mice (Fig. 6D). Our data verify that cleavage of GSL glycans from exosomes can sufficiently prevent the association of exosomes with A $\beta$ . This suggests that there may be multiple species of GSLs, especially sialylated forms, on exosomal membranes that organize into unique sites of high potency able to induce A $\beta$  binding and assembly.

In addition to gangliosides, cholesterol and sphingomyelin (SM) are also known to promote A $\beta$  assembly via the lateral packing of gangliosides on membranes (21,22). We found that both cholesterol and SM were highly abundant in exosomes compared with their parent cells (Fig. 7), suggesting that high densities of these two lipids would promote GSL binding to A $\beta$ . Another lipid, ceramide (Cer), which is the hydrophilic backbone of GSLs, is known to be involved in exosome generation (23). We found higher levels of ceramide in exosomes than in cells (Fig. 7), consistent with a previous report (23).

*Exosomes are incorporated into microglia in vitro and in vivo, in a GSL-glycan-independent manner* - Our previous in vitro experiments demonstrated that engulfment of exosomes by

mouse primary microglia occurred in a partially phosphatidylserine (PS)-dependent manner (8). However, deglycosylated proteins, e.g. immunoglobulin FC receptor, reportedly exhibit low affinity towards microglia (24). To determine whether cleavage of GSL-glycans would affect microglial uptake of exosomes, we exposed fluorescent-labeled exosomes pretreated with EGCCase or PBS, to microglial BV-2 cells. We found no decrease in microglial uptake of EGCCase-treated exosomes (Fig. 8A). Both of the labeled exosomes were co-localized with the microglial marker Iba1 when intracerebrally injected into mouse brains (Fig. 8B), and there were no obvious differences observed between untreated or EGCCase-treated exosomes. Few fluorescent exosomes were apparent in merged images of cells stained for either a neuronal or astroglial marker (Fig. 8C). The above data indicate that exosomes can be incorporated into microglia undisturbed by the absence of GSL-glycans on the membrane.

## DISCUSSION

Our study presented here clearly demonstrated that intracerebral exosome infusion leads to a decrease in A $\beta$  levels and ameliorates A $\beta$ -related pathologies in APP mice. In the mouse brains, A $\beta$  was trapped at the exosome surface by glycan moieties of GSLs and transported into microglia for degradation. Mass spectrometry-based analysis has revealed that GSLs are abundant in exosomes, compared to parental cells. Just how GSLs are packed so much more into the exosomes than in parental cells remains an unanswered question. Exosomes are produced by intraluminal budding of the limited membrane of endosomes. Accumulation of Cer, which is generated by the hydrolysis of SM, has been reported to initiate the budding (23). Cer can induce a coalescence of

small microdomains into larger microdomains to drive domain-induced budding of biological membranes (25), which results in highly loading Cer and its vicinal lipid molecules into the generated vesicle. Indeed, Cer and SM are concentrated in exosome membranes (Fig. 7) (23). In addition, SM forms a distinct membrane domain, namely a lipid raft, in the plasma membrane together with GSLs and cholesterol (26). Various raft-resident proteins have also been reported to be abundant in exosomes (27).

In the present study, providing GSLs-enriched exosomes to the APP mouse brains resulted in recovering synaptic impairment and decreasing A $\beta$  plaques. However, the effect of GSLs on AD pathogenesis is a controversial issue. GSL storage disorders, which are subtypes of lysosomal storage diseases caused by genetic dysfunction in GSL catabolism, share pathological features with AD, such as A $\beta$  burden (28,29). Accumulated gangliosides are observed in human brains exhibiting AD, and they are proposed to contribute to AD development through promoting A $\beta$  fibril formation (16). These discrepant effects of GSLs are likely to stem from their life span in brain tissues. Pathologically accumulated GSLs are pooled within cells to form complexes with A $\beta$  and its polymer (19,28), which might be retained to exert neuronal damages. On the other hand, exosomal GSLs capture A $\beta$  in extracellular fluid and are rapidly taken up by phagocytes without persistent harm to the brain.

Our present study demonstrated that exosomes derived from N2a cells can promote A $\beta$  fibril formation on their surface (Fig. 6A and B). The exosome-bound A $\beta$  was then incorporated into microglia for degradation (Fig. 1E, Fig. 8A and B)(8). Therefore, continuous infusion of exosomes induced a reduction in amyloid depositions in aged APP mouse brains (Fig. 3C). These results provide a notion that the exosomes in the brains

are rapidly cleared by microglia before the exosome-bound A $\beta$ s form amyloid fibrils for depositions. Amyloid plaques were reported to change their sizes over days in the brains of AD model mice (30). The exogenously added exosomes might prevent further A $\beta$  depositions by blocking the supply of the soluble A $\beta$ . Alternatively, exosomes might support the clearance of amyloid deposit, which already formed. The complex of GM1-A $\beta$  has reported to localize at the ends of extended A $\beta$  fibrils in the incubation mixture of GM1 and A $\beta$  (19). Alix, a marker for exosomes was enriched around the small A $\beta$  plaques in brain sections from AD patients (6). Similarly, once the exogenous exosome-associated A $\beta$ s are attached to the A $\beta$  fibrils in the amyloid plaques, they might provoke microglia gathering toward the plaques and accelerate their clearance.

Here, we used seed-free A $\beta$  to perform the A $\beta$  binding assay (Fig. 5D) and the SPR analysis (Fig. 5E and F) and demonstrated that A $\beta$ s directly bind to the exosomes through the GSL glycans on their surface. Seed-free A $\beta$  was reported to contain soluble species of A $\beta$ , but not insoluble amyloid forms (13). The GM1-A $\beta$  complex, which acts as a seed for A $\beta$  amyloidogenesis, is known to consist of a clustered GM1 and a monomeric A $\beta$  molecule (17, 31). Accordingly, our previous report have demonstrated that the exosomes derived from N2a cells almost prevented the oligomeric A $\beta$  formation from seed-free A $\beta$ , but not those preformed A $\beta$  oligomers, which are recognized by A11, a specific antibody against oligomer (8). Thus, the above findings suggested that the exosomes released from N2a cells would be mostly associated with monomeric A $\beta$  through their surface GSLs. However, a recent study demonstrated that soluble A $\beta$  oligomer strongly binds to GM1-containing membranes in vitro and in vivo, and GM1-bound A $\beta$  is detected in human

CSF (32). An additional investigation may be required in future to clarify which form of A $\beta$ s can be associated with the exosomes.

It is worth noting that other aggregate-prone proteins, including  $\alpha$ -synuclein and prion protein, which cause Parkinson's and Creutzfeldt-Jakob diseases, respectively, are also associated with exosomes (33,34). In addition,  $\alpha$ -synuclein and prion protein have been reported to associate with GSLs on the surface of synthetic liposomes (35,36). A challenging subject of future studies will be determining whether exosomes are involved in the clearance of these proteins.

The normal phagocytotic function of microglia is conceivably important for exosome-bound A $\beta$  clearance in this study. Increasing evidence has indicated that a large portion of secreted exosomes are convincingly taken up by microglia (8,37). In contrast, small amount of exosomes can be incorporated into neurons (38). If the clearance function of microglia is decreased or absent, then the exosome-bearing aggregate-prone proteins would trigger pathological events (i.e., formation of senile plaque) or even perform minor interneuronal transfer to propagate their toxic assemblies. Indeed, exosome-associated prion

proteins, in which their folded species are infectious, can spread between neuronal cells in a monoculture system (33). The transmissibility of amyloids, a characteristic feature of many neurodegenerative diseases including Alzheimer disease and spongiform encephalitis, might emerge under a lack of glial activity for removing exosomes.

Improvement of A $\beta$  clearance by exosome administration or enhancement of exosome generation provides a novel therapeutic approach for AD therapy. It is noteworthy that the A $\beta$ -degrading enzymes, IDE and neprilysin, have been reported to be found in exosomes secreted from microglia and adipose tissue-derived mesenchymal stem cells, respectively (39,40). Exosomes have been used as a delivery platform, encapsulating reagents or siRNAs (41,42). Peripheral injection of the exosomes holding siRNA (against an APP processing enzyme, BACE1) succeeded in brain targeting and specific gene knockdown in mice (41). In the future, development of engineered nanovesicles that regulate multiple processes in AD pathogenesis might be a valuable tool for the therapy.

## REFERENCES

1. Scheuner D., Eckman C., Jensen M., Song X., Citron M., Suzuki N., Bird T. D., Hardy J., Hutton M., Kukull W., Larson E., Levy-Lahad E., Viitanen M., Peskind E., Poorkaj P., Schellenberg G., Tanzi R., Wasco W., Lannfelt L., Selkoe D., and Younkin S. (1996) Secreted amyloid beta-protein similar to that in the senile plaques of Alzheimer's disease is increased in vivo by the presenilin 1 and 2 and APP mutations linked to familial Alzheimer's disease. *Nat. Med.* **2**, 864-870
2. Mawuenyega K. G., Sigurdson W., Ovod V., Munsell L., Kasten T., Morris J. C., Yarasheski K. E., and Bateman R. J. (2010) Decreased clearance of CNS  $\beta$ -amyloid in Alzheimer's disease. *Science* **330**, 1774
3. Hardy J, and Selkoe D. J. (2002) The amyloid hypothesis of Alzheimer's disease: progress and problems on the road to therapeutics. *Science* **297**, 353-356
4. Simons M., and Raposo G.(2009) Exosomes--vesicular carriers for intercellular communication. *Curr. Opin. Cell Biol.* **21**, 575-581
5. Vlassov A. V., Magdaleno S., Setterquist R., and Conrad R. (2012) Exosomes: current knowledge of their composition, biological functions, and diagnostic and therapeutic potentials. *Biochim. Biophys. Acta* **1820**, 940-948
6. Rajendran L., Honsho M., Zahn T. R., Keller P., Geiger K. D., Verkade P., and Simons K. (2006) Alzheimer's disease beta-amyloid peptides are released in association with exosomes. *Proc. Natl. Acad. Sci. USA* **103**, 11172-11177
7. Vingtdeux V., Hamdane M., Loyens A., Gele P., Drobeck H., Begard S., Galas M. C., Delacourte A., Beauvillain J. C., Buee L., and Sergeant N. (2007) Alkalinizing drugs induce accumulation of amyloid precursor protein by-products in luminal vesicles of multivesicular bodies. *J. Biol. Chem.* **282**, 18197-18205
8. Yuyama K., Sun H., Mitsutake S., and Igarashi Y. (2012) Sphingolipid-modulated exosome secretion promotes clearance of amyloid-beta by microglia. *J. Biol. Chem.* **287**, 10977-10989
9. Thery C., Amigorena S., Raposo G., and Clayton A. (2006) Isolation and characterization of exosomes from cell culture supernatants and biological fluids. *Curr Protoc. Cell. Biol.* **U3.22**, 1-29
10. DeMattos R. B., Bales K. R., Parsadanian M., O'Dell M. A., Foss E. M., Paul S. M., and Holtzman D. M. (2002) Plaque-associated disruption of CSF and plasma amyloid-beta (A $\beta$ ) equilibrium in a mouse model of Alzheimer's disease. *J. Neurochem.* **81**, 229-236
11. Mucke L., Masliah E., Yu G. Q., Mallory M., Rockenstein E. M., Tatsuno G., Hu K., Kholodenko D., Johnson-Wood K., and McConlogue L. (2000) High-level neuronal expression of abeta 1-42 in wild-type human amyloid protein precursor transgenic mice: synaptotoxicity without plaque formation. *J. Neurosci.* **20**, 4050-4058
12. Fujitani N., Furukawa J., Araki K., Fujioka T., Takegawa Y., Piao J., Nishioka T., Tamura T., Nikaido T., Ito M., Nakamura Y., and Shinohara Y. (2013) Total cellular glycomics allows characterizing cells and streamlining the discovery process for cellular biomarkers. *Proc. Natl. Acad. Sci. USA* **110**, 2105-2110
13. Naiki H., and Gejyo F. (1999) Kinetic analysis of amyloid fibril formation. *Methods Enzymol.* **309**, 305-318

14. Thery C. (2011) Exosomes: secreted vesicles and intercellular communications. *Fl1000 Biol Rep* **3**, 15
15. Grapp M., Wrede A., Schweizer M., Huwel S., Galla H. J., Snaidero N., Simons M., Buckers J., Low P. S., Urlaub H., Gartner J., and Steinfeld R. (2013) Choroid plexus transcytosis and exosome shuttling deliver folate into brain parenchyma. *Nat. Commun.* **4**, 2123
16. Ariga T., McDonald M. P., and Yu R. K. (2008) Role of ganglioside metabolism in the pathogenesis of Alzheimer's disease--a review. *J. Lipid Res.* **49**, 1157-1175
17. Utsumi M., Yamaguchi Y., Sasakawa H., Yamamoto N., Yanagisawa K., and Kato K. (2009) Up-and-down topological mode of amyloid beta-peptide lying on hydrophilic/hydrophobic interface of ganglioside clusters. *Glycoconj. J.* **26**, 999-1006
18. Yanagisawa K., Odaka A., Suzuki N., and Ihara Y. (1995) GM1 ganglioside-bound amyloid beta-protein (A beta): a possible form of preamyloid in Alzheimer's disease. *Nat. Med.* **1**, 1062-1066
19. Hayashi H., Kimura N., Yamaguchi H., Hasegawa K., Yokoseki T., Shibata M., Yamamoto N., Michikawa M., Yoshikawa Y., Terao K., Matsuzaki K., Lemere C. A., Selkoe D. J., Naiki H., and Yanagisawa K. (2004) A seed for Alzheimer amyloid in the brain. *J. Neurosci.* **24**, 4894-4902
20. Fujitani N., Takegawa Y., Ishibashi Y., Araki K., Furukawa J., Mitsutake S., Igarashi Y., Ito M., and Shinohara Y. (2011) Qualitative and quantitative cellular glycomics of glycosphingolipids based on rhodococcal endoglycosylceramidase-assisted glycan cleavage, glycoblotting-assisted sample preparation, and matrix-assisted laser desorption ionization tandem time-of-flight mass spectrometry analysis. *J. Biol. Chem.* **286**, 41669-41679
21. Yanagisawa K., and Matsuzaki K. (2002) Cholesterol-dependent aggregation of amyloid beta-protein. *Ann. N. Y. Acad. Sci.* **977**, 384-386
22. Yuyama K., and Yanagisawa K. (2010) Sphingomyelin accumulation provides a favorable milieu for GM1 ganglioside-induced assembly of amyloid beta-protein. *Neurosci. Lett.* **481**, 168-172
23. Trajkovic K., Hsu C., Chiantia S., Rajendran L., Wenzel D., Wieland F., Schwille P., Brugger B., and Simons M. (2008) Ceramide triggers budding of exosome vesicles into multivesicular endosomes. *Science* **319**, 1244-1247
24. Takata K., Hirata-Fukae C., Becker A. G., Chishiro S., Gray A. J., Nishitomi K., Franz A. H., Sakaguchi G., Kato A., Mattson M. P., Laferla F. M., Aisen P. S., Kitamura Y., and Matsuoka Y. (2007) Deglycosylated anti-amyloid beta antibodies reduce microglial phagocytosis and cytokine production while retaining the capacity to induce amyloid beta sequestration. *Eur. J. Neurosci.* **26**, 2458-2468
25. Gulbins E., and Kolesnick R. (2003) Raft ceramide in molecular medicine. *Oncogene* **22**, 7070-7077
26. Simons K., and Ikonen E. (1997) Functional rafts in cell membranes. *Nature* **387**, 569-572
27. de Gassart A., Geminard C., Fevrier B., Raposo G., and Vidal M. (2003) Lipid raft-associated protein sorting in exosomes. *Blood* **102**, 4336-4344
28. Keilani S., Lun Y., Stevens A. C., Williams H. N., Sjoberg E. R., Khanna R., Valenzano K. J., Checler F., Buxbaum J. D., Yanagisawa K., Lockhart D. J., Wustman B. A., and Gandy S. (2012) Lysosomal dysfunction in a mouse model of Sandhoff disease leads to accumulation of ganglioside-bound amyloid-beta peptide. *J. Neurosci.* **32**, 5223-5236
29. Xu Y. H., Barnes S., Sun Y., Grabowski G. A. (2010) Multi-system disorders of glycosphingolipid and ganglioside metabolism. *J. Lipid Res.* **51**, 1643-1675

30. Bolmont T., Haiss F., Eicke D., Radde R., Mathis C.A., Klunk W.E., Kohsaka S., Jucker M., and Calhoun M.E. (2008) Dynamics of the microglial/amyloid interaction indicate a role in plaque maintenance. *J. Neurosci.* **28**, 4283-4292
31. Matsuzaki K., Kato K., and Yanagisawa K. (2010) Abeta polymerization through interaction with membrane gangliosides. *Biochim. Biophys. Acta.* **1801**, 868-877
32. Hong S., Ostaszewski B.L., Yang T., O'Malley T.T., Jin M., Yanagisawa K., Li S., Bartels T., and Selkoe D.J. (2014) Soluble A $\beta$  oligomers are rapidly sequestered from brain ISF in vivo and bind GM1 ganglioside on cellular membranes. *Neuron* **82**, 308-319
33. Fevrier B., Vilette D., Archer F., Loew D., Faigle W., Vidal M., Laude H., Raposo G. (2004) Cells release prions in association with exosomes. *Proc. Natl. Acad. Sci. USA* **101**, 9683-9688
34. Emmanouilidou E., Melachroinou K., Roumeliotis T., Garbis S. D., Ntzouni M., Margaritis L. H., Stefanis L., and Vekrellis K. (2010) Cell-produced alpha-synuclein is secreted in a calcium-dependent manner by exosomes and impacts neuronal survival. *J. Neurosci.* **30**, 6838-6851
35. Martinez Z., Zhu M., Han S., and Fink A. L. (2007) GM1 specifically interacts with alpha-synuclein and inhibits fibrillation. *Biochemistry* **46**, 1868-1877
36. Sanghera N., Correia B. E., Correia J. R., Ludwig C., Agarwal S., Nakamura H. K., Kuwata K., Samain E., Gill A. C., Bonev B. B., and Pinheiro T. J. (2011) Deciphering the molecular details for the binding of the prion protein to main ganglioside GM1 of neuronal membranes. *Chem Biol* **18**: 1422-1431
37. Fitzner D, Schnaars M, van Rossum D, Krishnamoorthy G, Dibaj P, Bakhti M, Regen T, Hanisch UK, and Simons M (2011) Selective transfer of exosomes from oligodendrocytes to microglia by macropinocytosis. *J. Cell Sci.* **124**, 447-458
38. Fruhbeis C., Frohlich D., Kuo W.P., Amphornrat J., Thilemann S., Saab A.S., Kirchhoff F., Mobius W., Goebbels S., Nave K. A., Schneider A., Simons M., Klugmann M., Trotter J., and Kramer-Albers E. M. (2013) Neurotransmitter-triggered transfer of exosomes mediates oligodendrocyte-neuron communication. *PLoS Biol.* **11**, e1001604
39. Tamboli I.Y., Barth E., Christian L., Siepmann M., Kumar S., Singh S., Tolksdorf K., Heneka M.T., Lutjohann D., Wunderlich P., and Walter J. (2010) Statins promote the degradation of extracellular amyloid  $\beta$ -peptide by microglia via stimulation of exosome-associated insulin-degrading enzyme (IDE) secretion. *J. Biol. Chem.* **285**, 37405-37414
40. Katsuda T., Tsuchiya R., Kosaka N., Yoshioka Y., Takagaki K., Oki K., Takeshita F., Sakai Y., Kuroda M., and Ochiya T. (2013) Human adipose tissue-derived mesenchymal stem cells secrete functional neprilysin-bound exosomes. *Sci. Rep.* **3**, 1197
41. Alvarez-Erviti L., Seow Y., Yin H., Betts C., Lakhali S., and Wood M. J. (2011) Delivery of siRNA to the mouse brain by systemic injection of targeted exosomes. *Nat. Biotechnol.* **29**, 341-345
42. Zhuang X., Xiang X., Grizzle W., Sun D., Zhang S., Axtell R.C., Ju S., Mu J., Zhang L., Steinman L., Miller D., and Zhang H.G. (2011) Treatment of brain inflammatory diseases by delivering exosome encapsulated anti-inflammatory drugs from the nasal region to the brain. *Mol. Ther.* **19**, 1769-1779

Acknowledgements - This work was supported by Creation of Innovation Centers for Advanced Interdisciplinary Research Areas Program, Ministry of Education, Culture, Sports, Science and Technology, Japan. A part of this work was conducted at Hokkaido University, supported by "Nanotechnology Platform" Program of the Ministry of Education, Culture, Sports, Science and Technology (MEXT), Japan.

## FOOTNOTES

\*This work was supported by Creation of Innovation Centers for Advanced Interdisciplinary Research Areas Program, Ministry of Education, Culture, Sports, Science and Technology, Japan.

<sup>1</sup>To whom correspondence should be addressed: Tel: +81(11)-706-9001; FAX +81(11)-706-9087; E-mail: yigarash@pharm.hokudai.ac.jp

<sup>2</sup>The abbreviations used are: A $\beta$ , amyloid- $\beta$  peptide; AD, Alzheimer disease; APP, amyloid- $\beta$  precursor protein; GSL, glycosphingolipid; CTFs, C-terminal fragments; AICD, amyloid intracellular domain; N2a, Neuro2a; ECE, endothelin converting enzyme; IDE, insulin degrading enzyme; CTB, cholera toxin B subunit; EGCase, endoglycoceramidase

## FIGURE LEGENDS

**FIGURE 1. Exogenously injected exosomes trap A $\beta$  and are internalized into microglia in mouse brains.** Exosomes were isolated from culture supernatant of N2a cells by sequential centrifugation, eventually to 100,000g pellets. *A.* An electron microscopic image of phosphotungstic acid-stained exosomes. *B.* Exosomes were measured by dynamic light scattering. *C.* Exosomes were density-fractionated by sucrose gradient, and the fractions were analyzed by Western blotting to detect the exosome markers Alix, flotillin-1 (Flot-1), and ganglioside GM1 (GM1), as well as actin and A $\beta$ . CL; cell lysates. *D.* Biotinylated exosomes stereotaxically injected into the hippocampus of 4-month-old non-transgenic or APP mice were isolated using biotin-binding affinity beads, then analyzed by Western blotting to detect co-precipitated full-length (FL)-APP, A $\beta$ , and Alix. *E.* Conjugates of fluorescence-labeled A $\beta$  (green) and exosomes (red) were administered into the hippocampus of non-transgenic mice. The hippocampal images were captured 3 h after the injection, following antibody staining for the microglial marker Iba1 (blue). Scale bar, 50  $\mu$ m and 10  $\mu$ m (inset).

**FIGURE 2. Intracerebral administration of N2a-exosomes induces A $\beta$  clearance.** Exosomes (12  $\mu$ g protein/PBS/day) or vehicles were continuously infused into lateral ventricle (*A*, *C*, *D*) or right hippocampus (*B*) of APP mice (4 months) for 14 days. *A.* After the infusion, hippocampal levels of A $\beta$  were measured by enzyme-linked immunosorbent assay (ELISA). ( $n \geq 5$  animals per group; mean  $\pm$  SD, \* $p < 0.05$ , \*\* $p < 0.01$ ; Student's t test). *B.* Hippocampal A $\beta$  levels in ipsilateral and contralateral side were measured by ELISA. Values are represented as percentages of the A $\beta$  levels in the contralateral side. (PBS:  $n = 3$ , exosome:  $n = 4$ ; mean  $\pm$  SD, \*\* $p < 0.01$ ; Student's t test). *C.* Representative hippocampal sections of exosome- or vehicle-infused APP mice or age-matched nontransgenic controls, stained with

antibody against synaptophysin. MoDG, molecular dentate gyrus (DG); GrDG, granular DG; PoDG, polymorph DG. Scale bar, 100  $\mu\text{m}$ . *D*. Densities of synaptophysin-positive presynaptic terminals in the hippocampal sections in (*C*) were quantified (5 sections/mouse, 5 mice per group). Data presented are the mean $\pm$ SD, \*\*\* $p$ <0.001.

**FIGURE 3. Intracerebral administration of N2a-exosomes reduces A $\beta$  deposition.** Exosomes (12  $\mu\text{g}$  protein/PBS/day) were continuously infused into the hippocampus (*A-D*) or lateral ventricle (*E*) of 13-month-old APP mouse for 14 days. *A*. Representative image of APP mouse hippocampal section stained with antibody against A $\beta$  (4G8). DG, dentate gyrus. Scale bar, 200  $\mu\text{m}$ . *B*. A $\beta$ -immunopositive areas in each hippocampal region were quantified. ( $n = 4$  animals, three or four sections per mouse brain; \*\*\* $p$ <0.001). *C*. The number of ThS-positive plaques in each hippocampus was determined. ( $n = 4$  animals, two or three sections per a brain; \* $p$ <0.05). *D*. The levels of hippocampal A $\beta_{1-40}$  and A $\beta_{1-42}$  were measured by ELISA. ( $n = 3$  animals, assayed in duplicate; \*\* $p$ <0.01). *E*. Exosomes (Low, 12  $\mu\text{g}$  protein/PBS/day; High, 24  $\mu\text{g}$  protein/PBS/day) were infused. Hippocampal A $\beta$ s were measured by ELISA. ( $n \geq 4$  animals per group; \*\* $p$ <0.01 compared to PBS).

**FIGURE 4. Exogenous exosomes do not stimulate APP processing, expressions of A $\beta$ -degrading enzymes, or inflammatory response.** Exosomes or PBS were continuously infused into the lateral ventricles of APP mice (4-month-old) for 14 days (*A* and *B*).  $n \geq 5$  animals per group. *A*. Full-length (FL)-APP, APP-C-terminal Fragments (CTFs), and the A $\beta$ -degrading enzymes insulin-degrading enzyme (IDE), neprilysin (NEP), and angiotensin-converting enzyme (ACE) were detected in the hippocampus by Western blotting, and the intensity for each band was quantified. Data presented are the mean  $\pm$  SD. *B*. Expression levels of proinflammatory cytokines (IL-1 $\beta$ , IL-6, IFN- $\gamma$ , and TNF- $\alpha$ ) in the hippocampus were measured by ELISA. Data are mean  $\pm$  SD.

**FIGURE 5. Exosomal GSLs are responsible for A $\beta$  binding on the vesicles.** Exosomal and cellular glycomes of GSLs were surveyed by mass spectrometry. *A*. Total amounts of GSL-glycans in exosomes and their originating cells were determined by standardization with protein or phosphatidylcholine (PC) content. *B*. GSLs other than GM2 detected in exosomes or cells were classified according to the number of sialic acid moieties. *C*. Particle size of exosomes (untreated or treated with EGCase) was determined by dynamic light scattering analysis after incubating them at 37 $^{\circ}\text{C}$  for 0, 5, and 24 h. *D*. Representative images of A $\beta$  binding on N2a cells and exosomes (untreated as Ctrl, or treated with EGCase, red) after 5 h incubation with fluorescent A $\beta_{1-42}$  (1  $\mu\text{M}$ , green). The cells were stained with DAPI. Arrows indicate A $\beta$  fluorescence co-localized with exosomal signals. Scale bar, 25  $\mu\text{m}$  (N2a cells) and 10  $\mu\text{m}$  (exosomes) *E*. Surface plasmon resonance sensorgrams showing the interactions of N2a-derived exosomes (1  $\mu\text{g}$  protein/ $\mu\text{l}$ ) with immobilized A $\beta_{1-42}$  or A $\beta_{42-1}$ . The responses were subtracted from a blank surface prepared by ethanolamine deactivation *F*. Sensorgrams showing the interactions of the exosomes (untreated ctrl, or pretreated with EGCase, 1  $\mu\text{g}$  protein/ $\mu\text{l}$ ) with immobilized A $\beta_{1-40}$ , A $\beta_{1-42}$ , or A $\beta_{1-38}$ . The resultant responses were subtracted from a surface that was immobilized with bovine serum albumin (BSA).

**FIGURE 6. Exosomal GSLs are involved in A $\beta$  assembly.** *A.* Thioflavin fluorescence intensities were measured in mixtures of exosomes (untreated as Ctrl, or treated with EGCCase) incubated with 15  $\mu$ M A $\beta$ <sub>1-42</sub>. Data are presented as the mean  $\pm$  SD, \*\*\* $p$ <0.001 (n=4). *B.* Representative electron microscopic images of exosomes incubated for 5 h with 15 $\mu$ M A $\beta$ <sub>1-42</sub> are shown. Scale bar, 100 nm. *C.* The exosomes (untreated as Ctrl, or treated with EGCCase or sialidase) were incubated for 5 h with 15  $\mu$ M A $\beta$ <sub>1-42</sub>. The untreated exosomes were reacted with A $\beta$  in the presence of cholera toxin B subunit (CTB) or anti-GM2 antibody. Fluorescence intensities of thioflavin-T were then measured. Values in each column are the mean  $\pm$  SD of five values. \* $p$ <0.05, \*\* $p$ <0.01. *D.* Biotinylated exosomes (untreated as Ctrl, or treated with EGCCase), stereotaxically injected into the hippocampus of APP mice (4 months), were isolated at 3 h after the injection, and the levels of exosome-associated A $\beta$  were quantified by ELISA. Values are the mean  $\pm$  SD (n=4).

**FIGURE 7. Exosomal and cellular lipid analysis.** Levels of phosphatidylcholine (PC), cholesterol (Chol), sphingomyelin (SM), and ceramide (Cer) were measured in N2a cells and the isolated exosomes. The data presented are mean  $\pm$  SD from three independent experiments; \* $p$ <0.05, \*\* $p$ <0.01, \*\*\* $p$ <0.001.

**FIGURE 8. Cleavage of exosomal GSL-glycans does not affect their uptake by microglia.** *A.* Fluorescence-labeled exosomes (untreated as Ctrl, or treated with EGCCase) were exposed to microglial BV-2 cells for 3 h, and the fluorescence intensities of exosomes taken up into the cells were determined by confocal microscopy. *B.* Representative hippocampal sections of non-transgenic mice (4 months) injected with fluorescence-labeled exosomes (untreated as Ctrl, or treated with EGCCase, red) and stained with anti-Iba1 antibody. Arrows indicate significant exosomal fluorescence in Iba1-positive microglia. Scale bars, 50  $\mu$ m and 10  $\mu$ m (inserts). *C.* Hippocampal sections from non-transgenic mice (4-month-old) injected with fluorescence-labeled exosomes (untreated as Ctrl, or treated with EGCCase) stained with antibodies against the neuronal marker  $\beta$ III tubulin or the astroglial marker glial fibrillary acidic protein (GFAP). Bar, 50  $\mu$ m.

Table 1. Summary of GSL-glycans found in exosomes and their parental N2a cells

No.	Composition	Class	Name	Absolute quantity (pmol/mg protein)		Relative quantity (%)	
				Cells	Exosomes	Cells	Exosomes
1	(Hex)2(Neu5Ac)1	Gg	GM3	9.142	210.686	1.111	1.108
2	(Hex)2(HexNAc)1(Neu5Ac)1	Gg	GM2	693.815	16095.765	84.284	84.667
3	(Hex)2(HexNAc)1(Neu5Gc)1	Gg	GM2(Gc)	6.866	328.257	0.834	1.727
4	(Hex)2(Neu5Ac)2	Gg	GD3	0.000	5.067	0.000	0.027
5	(Hex)3(HexNAc)1(Neu5Ac)1	Gg	GM1	1.359	102.665	0.165	0.540
6	(Hex)3(HexNAc)1(Neu5Gc)1	Gg	GM1(Gc)	0.000	2.011	0.000	0.011
7	(Hex)3(HexNAc)1(Neu5Ac)2	Gg	GD1	0.833	489.823	0.101	2.577
8	(Hex)3	Gb	Gb3	0.000	883.100	0.000	4.645
9	(Hex)3(HexNAc)1	Gb	Gb4	1.884	4.378	0.229	0.023
10	(Hex)4(HexNAc)1-SSEA3	Gb	Gb5	3.684	0.000	0.448	0.000
11	(Hex)3(HexNAc)1	(n)Lc	(n)Lc4	12.654	198.461	1.537	1.044
12	(Hex)4(HexNAc)1	(n)Lc	Gal-(n)Lc4	3.684	24.117	0.448	0.127
13	(Hex)3(HexNAc)1(Fuc)2	(n)Lc	diFuc-(n)Lc4	0.000	9.987	0.000	0.053
14	(Hex)3(HexNAc)2(Fuc)1	(n)Lc	Fuc-(n)Lc5	0.922	7.729	0.112	0.041
15	(Hex)4(HexNAc)2	(n)Lc	nLc6	0.000	3.347	0.000	0.018
16	(Hex)5(HexNAc)2	(n)Lc		0.204	1.875	0.025	0.010
17	(Hex)4(HexNAc)2(Fuc)1(NeuAc)2	(n)Lc		0.337	0.000	0.041	0.000
18	(Hex)2(HexNAc)1	-	Lc3/aGM2	87.803	643.481	10.666	3.385
			<b>total</b>	823.189	19010.751	100.000	100.000

# Figure 1

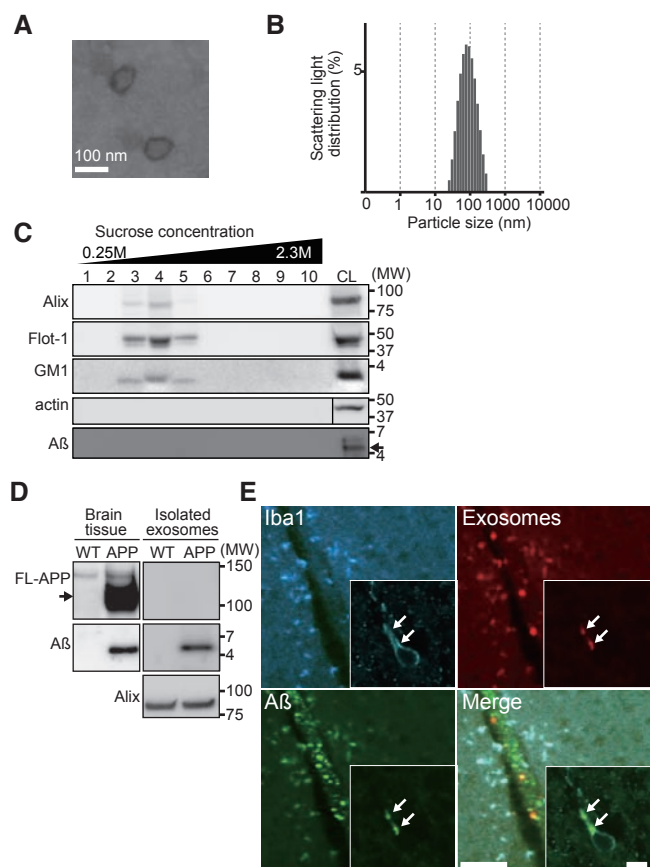


Figure 2

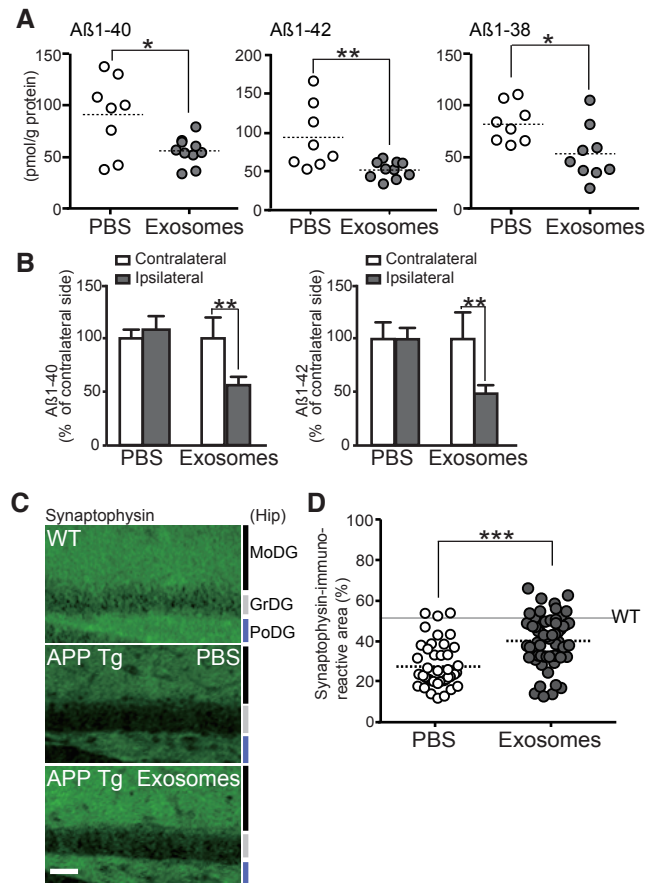


Figure 3

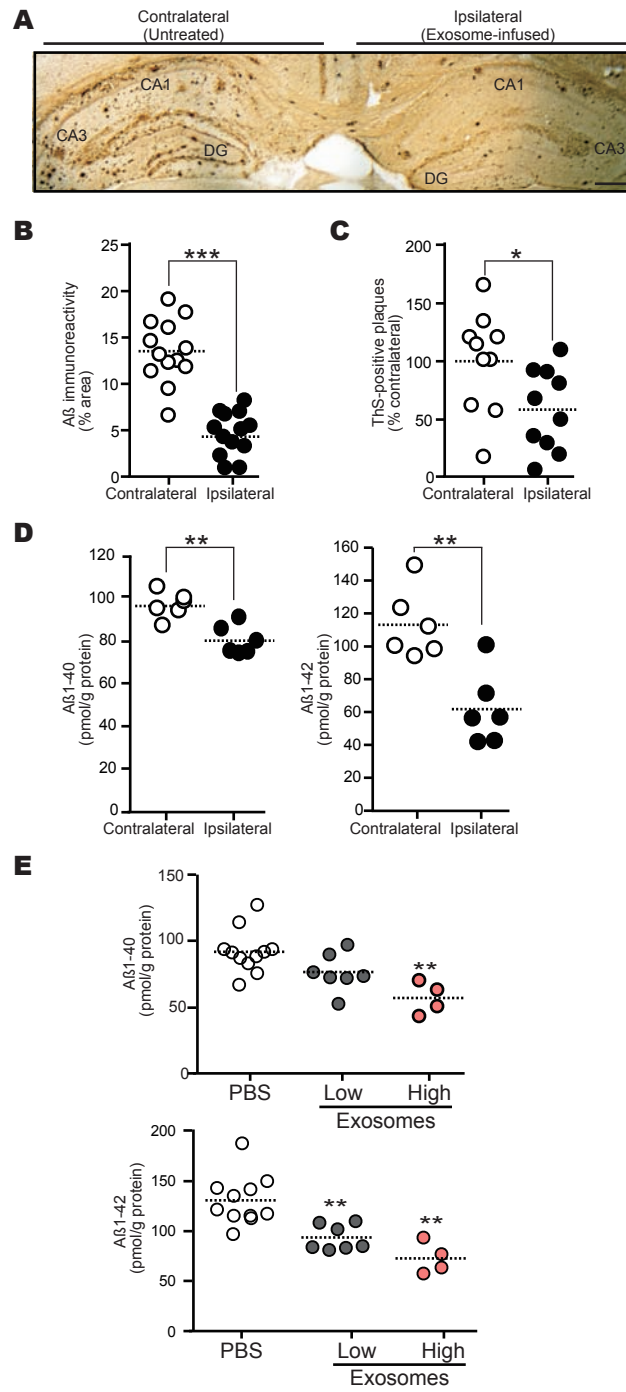


Figure 4

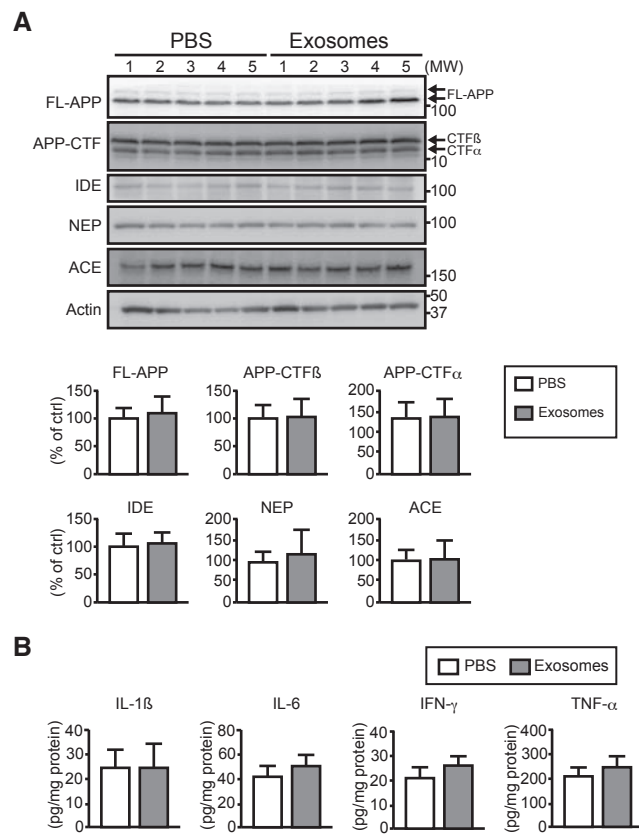


Figure 5

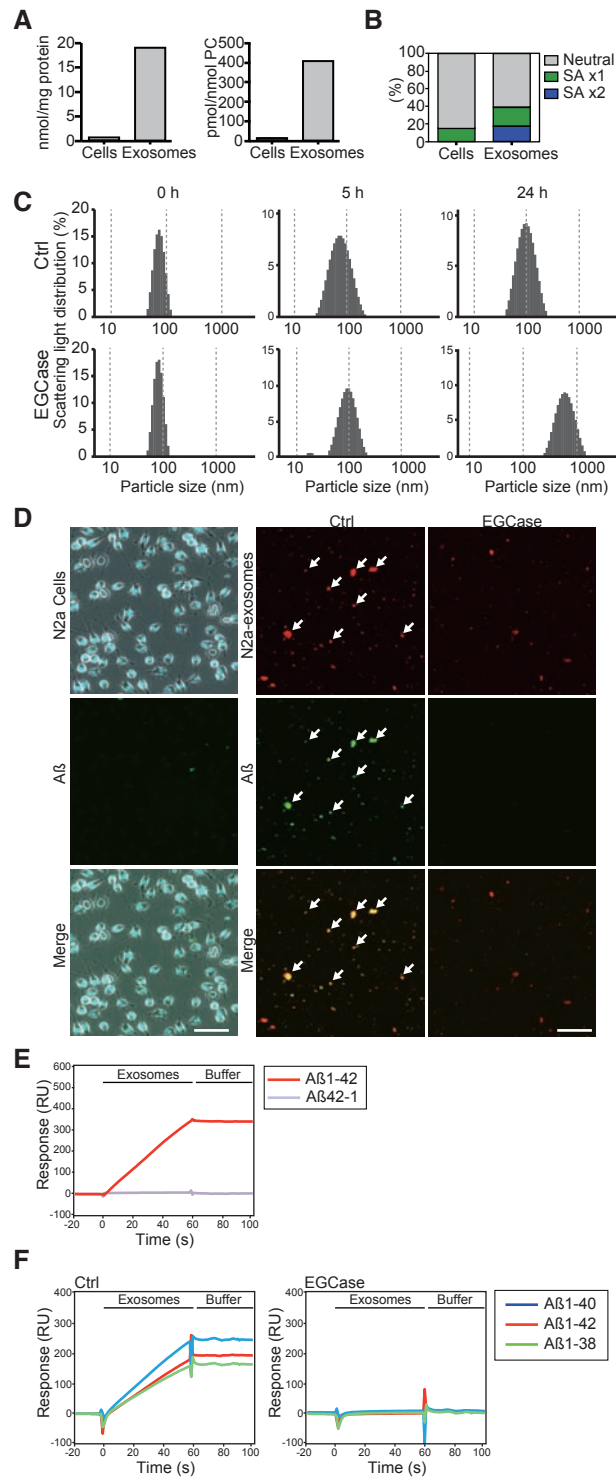


Figure 6

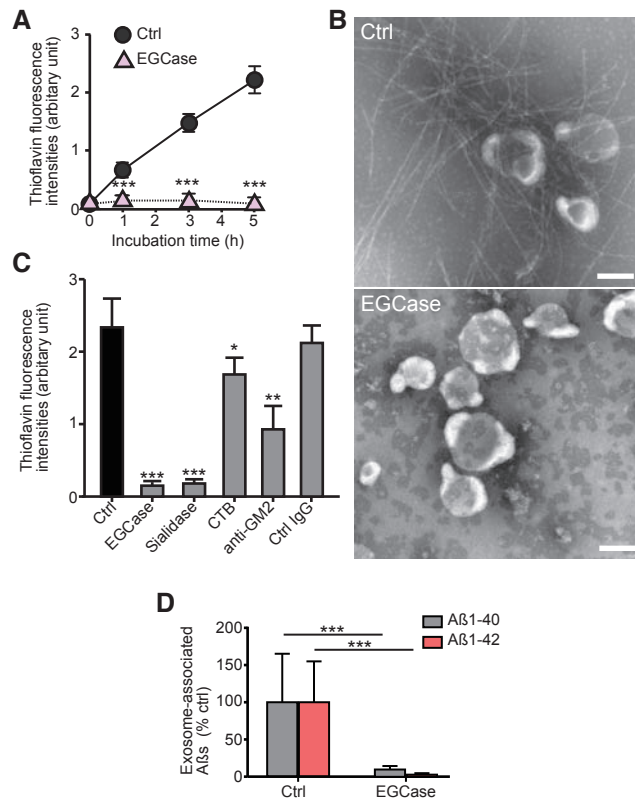


Figure 7

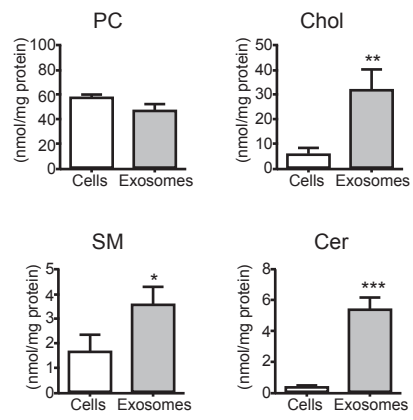


Figure 8

